Optical properties of ZnO nanocrystals embedded in BaF_2 film fabricated by magnetron sputtering

2007 J. Phys. D: Appl. Phys. 40 5598

(http://iopscience.iop.org/0022-3727/40/18/015)

IOP PUBLISHING JOURNAL OF PHYSICS D: APPLIED PHYSICS

J. Phys. D: Appl. Phys. **40** (2007) 5598–5601 doi:10.1088/0022-3727/40/18/015

Optical properties of ZnO nanocrystals embedded in BaF_2 film fabricated by magnetron sputtering

C H Zang[1,2], Y C Liu[3,6], R Mu[4], D X Zhao[5], J G Ma[5], J Y Zhang[5], D Z Shen[5] and X W Fan[5]

[1] Key Laboratory of Excited State Process, Changchun Institute of Optics, Fine Mechanics and Physics, Chinese Academy of Sciences, Changchun 130033, People's Republic of China
[2] Graduate School of Chinese Academy of Sciences, Beijing 100039, People's Republic of China
[3] Center for Advanced Optoelectronic Functional Materials Research, Northeast Normal University, Changchun 130024, People's Republic of China
[4] Center for Physics and Chemistry of Materials, Fisk University, Nashville, TN 37208, USA
[5] Key Laboratory of Excited State Process, Changchun Institute of Optics, Fine Mechanics and Physics, Chinese Academy of Sciences, Changchun 130033, People's Republic of China

E-mail: ycliu@nenu.edu.cn

Received 1 May 2007, in final form 24 June 2007
Published 30 August 2007
Online at stacks.iop.org/JPhysD/40/5598

Abstract

ZnO nanocrystals (NCs) embedded in a BaF_2 matrix have been prepared by a radio-frequency magnetron sputtering technique followed by a thermal annealing process from 400 to 1100 °C. X-ray diffraction results show that ZnO NCs with a hexagonal wurtzite structure are formed in a BaF_2 matrix. The average grain sizes are estimated ranging from 7.5 to 33 nm, corresponding to fabricated samples annealed at temperatures from 400 to 800 °C. Photoluminescence showed a very strong ultraviolet near-band-edge (NBE) emission located in the 364–383 nm spectral region. The emission intensity is enhanced and the linewidth is narrowed as the annealing temperature increases. The intensity ratio of ultraviolet NBE emission to deep-level visible is also increased with annealing temperature indicating that deep-level defects in ZnO are suppressed.

(Some figures in this article are in colour only in the electronic version)

ZnO is a direct band gap semiconductor with a band gap at ∼3.37 eV and a large excitonic binding energy of ∼60 meV [1]. It becomes a promising material of choice for efficient and stable UV-luminescent material at room temperature. ZnO nanocrystals (NCs) can lead to further blueshift of UV near-edge emission as a result of quantum confinement. Surface passivation and core–shell structured NCs can further enhance light emission intensity. The core–shell structured NCs are very attractive because of the possibility of obtaining unique optical, magnetic and catalytic properties [2]. High quality ZnO films can be prepared by many methods including pulse laser deposition [3], molecular beam epitaxy [4], sputtering [5] and ion implantation [6].

The magnetron sputtering technique has been proved to be an effective technique to fabricate ZnO NCs in SiO_2 and MgO [7,8] hosts. In this paper, we reported the first successful attempt to prepare ZnO NCs in a BaF_2 matrix by a radio-frequency magnetron sputtering method followed by thermal annealing. X-ray diffraction (XRD), photoluminescence and absorption spectra were used to evaluate the formation and the quality of ZnO NCs. The motivation to choose BaF_2 crystal as a host material was that BaF_2 (1) is a highly transparent ultraviolet window material with a band gap of 10.6 eV at 298 K [9], (2) is chemically stable and (3) has a low refractive index of 1.36. Because formed ZnO NCs with a refractive index $\sim n = 2.4$ [10] are embedded into BaF_2 matrices with a low refractive index to form a waveguide confined structure,

[6] Author to whom any correspondence should be addressed.

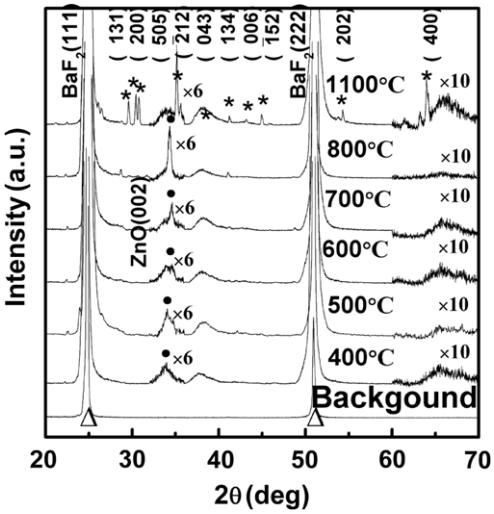

Figure 1. XRD spectra of samples annealed from 400 to 1100 °C. (The symbol (●) corresponds to the diffraction lines of ZnO (0 0 2), the symbol (▲) corresponds to the diffraction lines of BaF_2 (1 1 1) or BaF_2 (2 2 2), the symbol (∗) corresponds to the diffraction lines of Ba_2ZnO_3.)

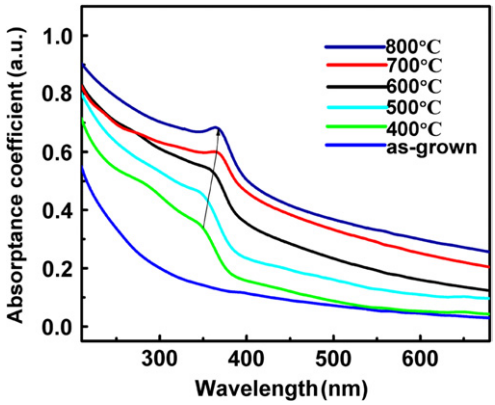

Figure 2. Absorption spectra of as-grown and samples annealed from 400 to 800 °C.

the luminescence from ZnO NCs can be effectively confined in the ZnO NCs to decrease the light loss.

Fabrication of ZnO NCs in a BaF_2 matrix can be summarized as follows: a highly transparent BaF_2 wafer was used as a substrate. A 90 mm BaF_2 wafer was used as the sputtering target. In addition, seven 10 mm ZnO circular targets were mounted on top of BaF_2 with equal spacing. The base pressure for the sputtering was below 2×10^{-5} Torr. The target–substrate distance was 50 mm. The substrate temperature was controlled at 300 °C. The working pressure in the chamber was kept at 7×10^{-3} Torr during the film growth. The rf power was kept at 180 W. Ultra-pure (5N) Ar gas was introduced into the sputtering chamber through a mass flow control system at a rate of 60 SCCM. After 1.5 h sputtering the deposited film thickness was estimated to be ∼1 μm. The as-grown film on BaF_2 was then cut into several pieces for further thermal treatments. Each sample was then annealed at a preset temperature ranging from 400 to 800 °C for 20 min under N_2 atmosphere. After annealing the samples were characterized with a D/max-RA x-ray spectrometer (Rigaku), a UV-Vis spectrophotometer and a micro-photoluminescence (PL) spectrometer excited with a He–Cd laser at 325 nm.

Figure 1 shows XRD patterns of samples annealed from 400 to 1100 °C. In addition to two very strong peaks due to (1 1 1) and (2 2 2) of the BaF_2 substrate, two broad bands were also observed at 34° and 38°. There was another very broad band at ∼65.5° with a shoulder at ∼68°. It is known that the peak at ∼34° represents the ZnO NCs in the film. The peak at ∼65.5° could be due to the BaF_2 matrix with an (3 3 1) orientation. The shoulder at ∼68° may come from ZnO with (1 1 2) and/or (2 0 1) orientations. XRD data suggest that we may form ZnO and BaF_2 nanocomposite materials. Since the overall concentration of ZnO in the film is only a few per cent, the formed ZnO NCs are expected to be embedded in a BaF_2 matrix. As the annealing temperature increased to 500 °C, ZnO with (1 1 2) orientation was clearly observed at ∼67.5°. However, when the annealing temperature reached 600 °C, the band at ∼67.5° disappeared and the ZnO NC diffraction peak at ∼34° split into two peaks such that one peak was at 34° and the other one was at 34.5°. When the annealing temperature reached 700 °C, a sharp peak was observed at 34.52 °C; it suggests that the formed ZnO NCs had a preferred (0 0 2) orientation. It is known that the peak position of (0 0 2) orientation for bulk crystals should be at 34.42° [11]; however, the measured diffraction peak (0 0 2) of ZnO NCs from this experiment was located at ∼34°–34.52°. The slight shift may be attributed to the stress from the BaF_2 matrix because of the big lattice mismatch between ZnO and BaF_2. To evaluate the mean grain size of ZnO NCs, the Scherrer formula was used: $d = 0.9\lambda/B\cos(\theta_B)$, where λ, θ_B, B are the x-ray wavelength (0.154 nm), the Bragg diffraction angle and the linewidth at half maximum of the diffraction peak around 34.42°, respectively. The calculated mean particle sizes were 7.54 nm, 8.66 nm, 14.7 nm, 19.36 nm and 33 nm for the annealing at 400 °C, 500 °C, 600 °C, 700 °C and 800 °C, respectively. In order to identify the peak at ∼38°, we increased the annealing temperature from 800 to 1100 °C. When the annealing temperature reached 800 °C, a sharp peak was observed at 34.2 °. It suggests ZnO NCs were formed with (0 0 2) orientation. Some new peaks were observed at the same annealing temperature. When the annealing temperature reached 1100 °C, the peak at ∼34.2° disappeared and a series of new peaks turned out. It was tentatively identified to be due to the structure of Ba_2ZnO_3. The peaks at ∼29.6°, 30.47°, 30.8°, 35.1°, 38°, 41.2°, 43.1°, 44.9°, 54.4° and 64° may be Ba_2ZnO_3 with (1 3 1), (2 0 0), (5 0 5), ($\bar{2}$ 2 1), (0 4 3), (1 3 4), (0 0 6), ($\bar{1}$ 5 2), (2 0 2) and (4 0 0) orientations, respectively. From 400 to 1100 °C, the peak at ∼38° did not change obviously. We referred to the decomposing temperature of $BaZnF_4$ at ∼745 °C, ZnF_2 at ∼875 °C [12] and the formation temperature of Ba_2ZnO_3 ranging from 1000 to 1400 °C; so we attempted to assign it to the diffraction lines of Ba_2ZnO_3. The formation temperature of Ba_2ZnO_3 ranges from 1000 to 1400 °C, which was 200 °C at least higher than that of Ba_2ZnO_3 in this work. The reason is that nano-ZnO particles with a large number of surface atoms have high surface free energy to facilitate interface reactions. As a result the formation temperature of Ba_2ZnO_3 decreased by the interfacial reaction of nano-ZnO and BaF_2 particles in this work.

Figure 2 shows the absorption spectra of as-grown and samples annealed from 400 to 800 °C. The very weak

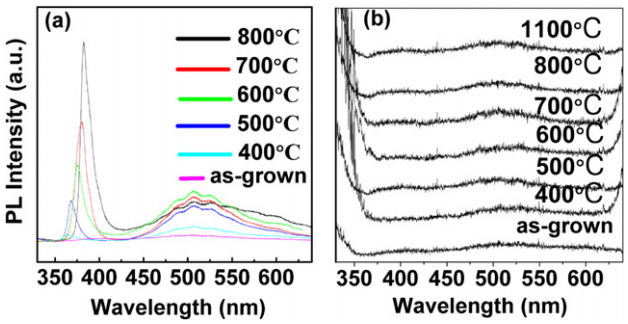

Figure 3. (*a*) Room temperature PL spectra of as-grown sample and samples annealed from 400 to 800 °C. (*b*) Room temperature PL spectra of BaF_2 film grown on the BaF_2 matrix annealed from 400 to 1100 °C and as-grown samples.

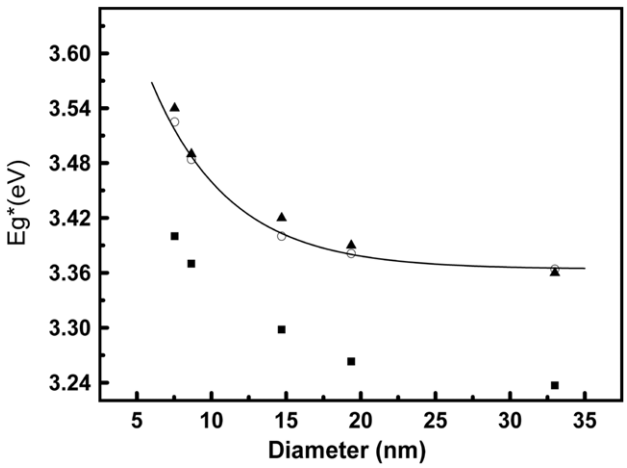

Figure 4. The dependence of the band gap enlargement versus the ZnO NCs diameter as calculated from the effective mass model (○) and the corresponding experimental data of UV emission peak (■) and the absorption onset (▲).

absorption was from small sized ZnO and clusters embedded into BaF_2 matrices. For the as-grown sample at 300 °C, ZnO NCs cannot be formed. When the annealing temperature increased to 400 °C, the exciton absorption peak at ∼349 nm started to appear. Then, the absorption peak intensity was further enhanced with a slight redshift as the temperature increased. Qualitatively, the weakening of the quantum confinement effect may explain the redshift of the exciton absorption peak. The observation of the distinct exciton absorption feature in the ZnO NCs embedded in BaF_2 is attributed to the large exciton binding energy of ZnO itself of ∼60 meV.

Figure 3(*a*) shows room temperature PL spectra of as-grown and samples annealed at different temperatures. For the as-grown sample, two emissions could be detected at positions of ∼400 and ∼505 nm, although they were very weak. The two bands could be assigned to a possible Zn ion replacing the Ba ion site [13] and deep level emission. As the annealing temperature increased from 400 to 800 °C, ZnO NCs started to form in the N_2 atmosphere, two major bands were observed. The former was due to free and bound exciton emission while the latter deep-level emission was attributed to the presence of the impurities and structured defect emissions of ZnO NCs [14–16]. When the temperature was above 500 °C, UV emission gradually become strong, the linewidth narrowed. The peak position redshifted from 364 to 383 nm. The FWHM measured are ∼158 meV, 102 meV, 100 meV, 106 meV and 101 meV, respectively, for the samples annealed at 400 °C, 500 °C, 600 °C, 700 °C and 800 °C. When the annealing temperature reached 800 °C, a kind of $Ba_x(Zn_yO_{(x+y)})$ structure substance was formed. It could decrease the surface defects of ZnO particles, so the deep-level emission was relatively low. The PL intensity ratio of UV emission to the deep-level green emission was not so high as in that grown by ion implantation [10] or MBE [4]. The impact of magnetron sputtering and the difference in thermal expansion and stress may cause interface defects [17], although the stress may decrease during the thermal process. In figure 3(*a*) the UV near-band emission peak was redshifted 169 meV to the low energy side with an increase in the grain size from 7.5 to 33 nm corresponding to the annealing temperature from 400 to 800 °C. The particle size dependence on the shift of the exciton emission peak is expected to be mainly due to a quantum-confinement-induced energy gap enhancement. Figure 3(*b*) shows the BaF_2 film grown on the BaF_2 matrix annealed from 400 to 1100 °C and as-grown samples. There was no obvious luminescence, which can by reference to figure 3(*a*) explain the PL caused by ZnO NCs.

The relationship between the band gap and the size of NCs can be obtained using the effective mass model. The band gap E_g^* (eV) can be approximately written as

$$E_g* = E_g^{\text{bulk}} + \frac{\hbar^2\pi^2}{2er^2}\left(\frac{1}{m_e^*} + \frac{1}{m_h^*}\right) - 0.248E_{\text{Ryd}}^* \text{ [18]}, \quad (1)$$

where E_g^{bulk}, $\hbar$, r and E_{Ryd}^* are the bulk energy gap, the Plank constant, the radius of NCs and the exciton binding energy, respectively. Taking $E_g^{\text{bulk}} = 3.37$ eV, the electron and the hole effective mass are $m_e^* = 0.24m_0$ and $m_h^* = 0.45m_0$ [7,19], using the bulk exciton binding energy $E_{\text{Ryd}}^* = 60$ meV without considering the increase in exciton binding energy due to the weak confinement.

Figure 4 shows the energy corresponding to both the UV near-band-edge (NBE) emission peaks, the absorption onset and the dependence of the band gap enlargement on the ZnO NCs diameter as calculated from the effective mass model (equation (1)). The energy corresponding to the UV emission peak and absorption peak has the same tendency, which indicates the size-dependent energy gap. The absorption data fit well with the curve theoretical calculated from the effective mass model. However, the PL peak does not coincide with the theoretical curve; this is because the UV NBE emission is due to the overlapping of the free and the bound exciton emission. The bound exciton is attributed to the interface defects of ZnO NCs embedded in BaF_2; thus the PL peaks have a large deviation from the theoretical calculated value. In addition, the binding energy of the exciton should be taken into consideration.

Figure 5 shows the room temperature PL spectra of the sample annealed at 1100 °C. The emission at ∼376 nm was assigned to UV near-band emission of ZnO nano-particles core surrounded by the Ba_2ZnO_3 nano-particles shell; the core became small causing the blueshift of UV near-band

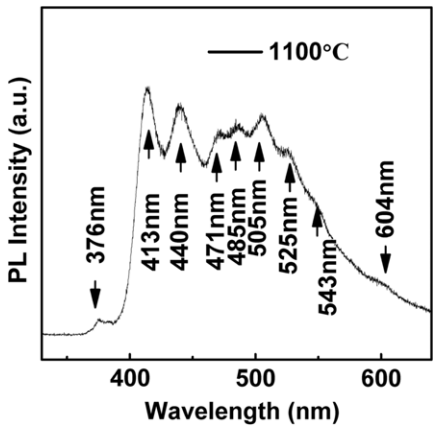

Figure 5. Room temperature PL spectra of sample annealed at 1100 °C.

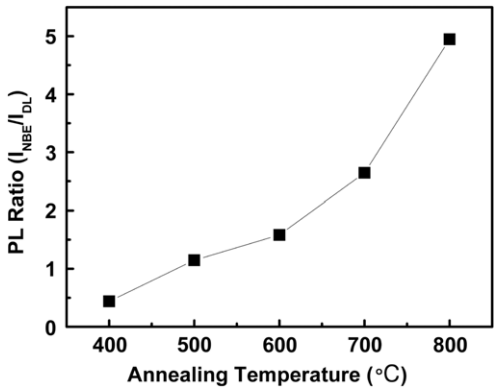

Figure 6. The intensity ratio of the UV NBE emission to the deep-level emission for the samples annealed from 400 to 800 °C.

emission and the weak intensity of UV near-band emission was attributed to the disorder of ZnO (core) and Ba_2ZnO_3 (shell) nano-particles interface region. Furthermore, the high temperature annealing may cause the F ion to diffuse into ZnO to form an impurity energy level related to F in the ZnO energy gap. A series of peaks of deep-level emissions were observed. The emission at ∼413 nm was argued to be the results of F_n centre formation at higher temperature [10], the emissions at 505 nm and 525 nm were attributed to the deep-level defects and the emissions at 543 nm and 604 nm were assigned to the F_A-centre and the F-centre, respectively [20]. The emission at ∼471 nm was characteristic of the traps present in the ZnO NCs; the one at ∼440 nm was attributed to the emission of ZnO surface states. It is difficult to identify the origin of the emissions at ∼485 nm. Figure 6 shows that the PL intensity ratio of the UV emission to the deep-level green emission increased as the annealing temperature increased from 400 to 800 °C. It illustrates that the concentrations of the defects related to the deep level emission tend to reduce as the annealing temperature increases.

In conclusion, it is for the first time that ZnO NCs embedded in the BaF_2 matrix with (0 0 2) preferential orientation were synthesized by the magnetron sputtering method. The impact of sputtering and thermal expansion may cause disorderly arranged areas and boundaries between ZnO and BaF_2 NCs. It could be more likely responsible for the surface defects. As the annealing temperature increases from 400 to 800 °C, the grain size increases from 7.5 to 33 nm and the UV emission peak is redshifted by 169 meV; the UV emission peak position redshifts from 364 to 383 nm. The quantum confinement effect plays an important role in the energy gap enhancement. The PL spectra show that the UV emission intensity increases and the deep-level green emission intensity decreases relatively (for the sample at 800 °C); its FWHM decreases from 158 to 101 meV. These results indicate that high-quality ZnO NCs embedded in BaF_2 are formed.

Acknowledgments

This work is supported by the National High Technology Research and Development Program of China (2006AA03Z311), the National Natural Science Foundation of China Grant No 60576040 and the Cultivation Fund of the Key Scientific and Technical Innovation Project, Ministry of Education of China No 704017. RM would like to acknowledge the partial financial support from the NSF-CREST CA:HRD-0420516 and the NSF-STC CLiPS under Grant 0423914.

References

[1] Zeuner A, Alves H, Hofman D M, Meyer B K, Heuken M, Blasing J and Krost A 2002 *Appl. Phys. Lett.* **80** 2078
[2] Li J, Zeng H, Sun S H, Liu J P and Wang Z L 2004 *J. Phys. Chem.* B **108** 14005
[3] Ryu Y R, Zhu S, Budai J D, Chandrasekhar H R, Miceli P F and White H W 2000 *J. Appl. Phys.* **88** 201
[4] Chen Y, Bragnall D M, Koh H J, Park K T, Hiraga K, Zhu Z and Yao T 1998 *J. Appl. Phys.* **84** 3912
[5] Kim K K, Song J H, Jung H J and Choi W K 2000 *J. Appl. Phys.* **87** 3573
[6] Zeng H, Cai W, Cao B, Hu J, Li Y and Liu P 2006 *Appl. Phys. Lett.* **88** 181905
[7] Ma J G, Liu Y C, Xu C S, Liu Y X, Sao C L, Xu H Y, Zhang J Y, Lu Y M, Shen D Z and Fan X W 2005 *J. Appl. Phys.* **97** 103509
[8] Ma J G, Liu Y C, Shao C L, Zhang J Y, Lu Y M, Shen D Z and Fan X W 2005 *Phys. Rev.* B **71** 125430
[9] Rodnyi P A, Stryganyuk G B, van Eijk C W E and Voloshinovskii A S 2005 *Phys. Rev.* B **72** 195112
[10] Liu Y C, Xu H Y, Mu R, Henderson D O, Lu Y M, Zhang J Y, Fan X W and White C W 2003 *Appl. Phys. Lett.* **83** 1210
[11] Gupta and Mansingh A 1996 *J. Appl. Phys.* **80** 1063
[12] Shojiya M, Kawamoto Y, Konishi A and Wakabayashi H 2000 *Thin Solid Films* **358** 99
Shojiya M, Kawamoto Y, Konishi A and Wakabayashi H 2000 *Thin Solid Films* **358** 103
[13] Staebler D L and Schnatterly S E 1971 *Phys. Rev.* B **3** 516
[14] Vanheusden K, Warren W L, Seager C H, Tallant D R, Voigt J A and Gnade B E 1996 *J. Appl. Phys.* **79** 7983
[15] Hu J Q and Bando Y 2003 *Appl. Phys. Lett.* **82** 1401
[16] Studenikin S A and Cocivera M 2002 *J. Appl. Phys.* **91** 5060
[17] Chen Z Q, Maekawa M, Kawasuso A, Sakai S and Naramoto H 2006 *J. Appl. Phys.* **99** 093507
[18] Zhang X H, Chua S J, Yong A M, Chow S Y, Yang H Y, Lau S P and Yu S F 2006 *Appl. Phys. Lett.* **88** 221903
[19] Lin K-F, Cheng H-M, Hsu H-C, Lin L-J and Hsieh W-F 2005 *Chem. Phys. Lett.* **409** 208–11
[20] Chen J, Lin L-B and Jing F-Q 2002 *Nucl. Instrum. Methods Phys. Res.* B **187** 354–60